Tissue-specific cells generated to predict xenogeneic immune responses demonstrate that SLA-downregulated kidney proximal tubular epithelial cells are low immunogenic

Katharina Schmalkuche
Institute of Transfusion Medicine and Transplant Engineering, Hannover Medical School

Reinhard Schwinzer
Transplantation Laboratory, Clinic for General, Visceral and Transplantation-Surgery, Hannover Medical School

Nadine Wenzel
Institute of Transfusion Medicine and Transplant Engineering, Hannover Medical School

Emilio Valdivia
Institute of Transfusion Medicine and Transplant Engineering, Hannover Medical School

Björn Petersen
Department of Biotechnology, Institute of Farm Animal Genetics, Friedrich-Loeffler-Institute, Federal Research Institute for Animal Health

Rainer Blasczyk
Institute of Transfusion Medicine and Transplant Engineering, Hannover Medical School

Constanca Figueiredo (Figueiredo.Constanca@mh-hannover.de)
Institute of Transfusion Medicine and Transplant Engineering, Hannover Medical School

---

Article

Keywords: SLA, RNAi, kidney xenotransplantation

Posted Date: February 10th, 2023

DOI: https://doi.org/10.21203/rs.3.rs-2519870/v1

Abstract

Patients with kidney failure depend on transplantation as the only curative option. Xenotransplantation re-emerged as a promising alternative to enlarge the available organ pool. However, the success of xenotransplantation depends on the design and selection of specific genetic modifications and on the development of robust assays allowing for a precise assessment of tissue-specific immune responses. Nevertheless, cell-based assays are often compromised by the low proliferative capacity of primary cells. Proximal tubular epithelial cells (PTECs) play a crucial role in kidney function. Here, we immortalized PTEC (imPTEC) by overexpression of simian virus 40 T large antigen. imPTEC showed typical morphology, phenotype, and functionality, but maintained steady cell cycling rates. Furthermore, SLA class I and class II transcript levels were reduced by up to 85% after transduction with lentiviral vectors encoding for shRNAs targeting β2-microglobulin and the class II transactivator. This contributed to reduce xenogeneic T-cell cytotoxicity ($P = 0.0069$) and decrease pro-inflammatory cytokine secretion such as IL-6 and IFN-γ. This study showed the feasibility to generate highly proliferative renal tubular cells and the development of tissue-specific immunomonitoring assays. Silencing SLA expression on PTEC demonstrated to be an effective strategy to prevent xenogeneic cellular immune responses and may strongly support graft survival after xenotransplantation.

Introduction

The kidney regulates vital processes such as the regulation of blood pressure, osmoregulation, or the maintenance of the acid-base balance [1]. Thus, patients suffering from end-stage kidney disease (ESRD) rely on dialysis or the highly desirable kidney transplantation (KTx) as the most effective treatment option. However, both scarcity of organs and genetic disparities between donor and recipient mainly on human leukocyte antigen loci often lead to long waiting times until KTx [2–5]. Currently, a mortality rate of 15% is observed in patients waiting on average 3.9 years for a suitable organ [6]. Kidney xenotransplantation may represent a promising alternative to circumvent the shortage of human organs. Nevertheless, genetic differences between pigs and humans trigger severe immune responses contributing to graft failure and rejection. Recently, life-sustaining pig kidney xenografts were proven to survive for approximately 500 days and orthotropic heart xenografts for up to 200 days in non-human primates [7]. In addition, as a remarkable milestone, the first genetically modified porcine heart and kidney were transplanted into a human, however, the patients survived only weeks to months after xenotransplantation [8,9].

Hence, the development of robust assays to predict the strength of xenogeneic immune responses targeting kidney cells are crucial to support the development of kidney xenotransplantation. Proximal tubular epithelial cells (PTECs) are extensively involved in renal clearance and tissue regeneration after injury or inflammation, and they are essential for the recovery of important metabolites by active transport [10–12]. Besides the endothelium, renal tubular epithelial cells show relevant immunoregulatory functions during immune rejection after KTx [13]. Therefore, in this study, we focused on evaluating the

feasibility to generate and use immortalized PTEC (imPTEC) to investigate the impact of specific genetic modifications on the strength of the immune response. PTECs play an essential role in kidney function and their use for the development of specific in vitro assays may become central in the evaluation of xenograft survival after transplantation. However, freshly isolated PTEC proliferation capability is limited, which means that they are unsuitable for routine testing or require the use of additional animals to obtain sufficient cellular material. Hence, the establishment of PTEC lines would facilitate the development of in vitro assays in different diagnostic and research areas to evaluate the feasibility and efficiency of new therapeutic strategies to reduce and optimize the need for experimental animals.

Results

3.1 Immortalized PTECs maintain typical cell morphology

After immortalization of porcine PTECs (imPTEC) with lentiviral vectors harboring the complete SV40 large T-antigen (ag) gene sequence (Fig. 1a), stable high levels of SV40 large T-ag transcripts were detected in several passages (0.94 ± 0.05 (passage 5), 1.05 ± 0.17 (passage 10), 1.02 ± 0.11 (passage 15), 0.71 ± 0.13 (passage 20) and 0.99 ± 0.24 (passage 25)) (Fig. 1b). mCherry-positive populations were isolated by cell sorting with a purity of 99.73% ± 0.24 ($P < 0.0001$) and expanded to generate cell lines (Fig. 1c, d,e).

The expression of the PTEC-specific markers aquaporin-1 (AQP-1), sodium/potassium-transporting ATPase subunit alpha-1 (ATP1A1), and tight junction protein-1 (ZO-1) showed no significant differences between primary and immortalized cells (Fig. 2a-c). Frequencies of protein expression of AQP1, ATP1A1, and ZO-1 in primary PTECs were 99.10% ± 0.78, 98.10% ± 0.29, 98.60% ± 0.85, and in imPTECs were 99.77% ± 0.13, 97.93% ± 2.33, 96.98% ± 1.67, respectively (Fig. 2b). These data suggest that transduction and cell immortalization does not affect PTECs phenotype.

3.2 Proliferation rate and cell cycle analysis

Immediately after passage 3, imPTEC proliferation rate was significantly ($P = 0.0029$) increased compared to primary PTECs. The population doubling time of primary PTECs was 11.0 ± 0.82 days in comparison to 6.67 ± 0.47 days of imPTECs. Also after passage 6, significantly higher proliferation rates ($P = 0.0078$) of imPTECs in comparison to native PTECs were observed. Primary PTECs required 30.67 ± 4.99 days to increase their number by 12-fold of the initial number. In contrast, imPTECs showed a 12-fold cell number increase of 12.67 ± 1.25 days after transduction. In fact, the imPTECs population doubled on average within 2 days and remained unaltered by passage 20, in contrast to the primary cells where the doubling rate decreased with an increasing number of passages (Fig. 3a).

Cell cycle analysis of PTECs in lower passage numbers revealed frequencies of 73.85% ±0.80 of primary PTECs in G1 in comparison to 80.59% ± 2.04 imPTECs shortly after transduction (passage 2). Higher frequencies of primary cells were in the S phase of the cell cycle in comparison to imPTECs (11.55% ±

0.05 vs 7.67% ± 0.21, P < 0.0001) were observed. Similarly, 14.60% ± 0.80 of primary PTECs and 10.73% ± 0.60 of imPTECs (P = 0.0048) were detected in the G2/M phase of the cell cycle (Fig. 3b,c). Remarkably, in higher passages (passage 10) and as expected, an increased frequency of imPTECs was detected in the G2 phase and lower frequencies of cells in the G1 phase. Compared to the primary cells (G1 phase: 89.32% ± 0.57, S phase: 5.27% ± 0.25, and G2 phase: 5.40% ± 0.39), the imPTECs were represented by 76.79% ± 0.72 (P < 0.0001) in G1 phase, 8.902% ± 0.30 (P < 0.0001) in the S phase and 14.30% ± 0.62 (P < 0.0001) in the G2/M phase (Fig. 3d,e). These results indicate that the majority of primary PTECs remain at higher passages in the G1 phase, while the cell cycle of immortalized cells remains almost unaffected in later passages.

3.3 Immortalized PTECs are functional

Epithelial cells play a crucial function during wound healing processes. In particular proliferation and migration are important mechanisms during tissue repair [14] Therefore, the migratory ability of PTEC was used to evaluate the functionality of imPTEC lines in scratch assays. After 24 hours, imPTECs (passage 2) completely closed the scratch, whereas primary cells migrated slowly and only overgrew the gap after 36 hours (Fig. 4a). This difference became even more obvious when analyzing the migration capability at higher passages (passage 10). Primary PTECs at passage 10 were not capable to close the scratch even after 48 hours, whereas immortalized cells formed a confluent monolayer after 24 hours (Fig. 4b).

3.4 Silencing SLA class I and class II expression by genetic engineering immortalized PTECs

The use of xenogeneic organs as an alternative to increasing the pool of organs suitable for transplantation is associated with the necessity of genetic modification to overcome immunological barriers posed by phylogenetic discrepancies between pigs and humans. One of the strategies proposed to reduce xenograft immunogenicity is the downregulation of SLA class I and class II expression [15]. A robust silencing of SLA class I and class II expression may decrease the strength of allo- or xenogeneic immune responses by generating an immunologically invisible status of tissues and organs supporting graft survival [16–18]. The use of PTEC isolated from genetically modified pigs or in vitro genetically modified PTEC may contribute to evaluating the effect of specific genetic modifications in the human immune response towards porcine-derived kidneys and to monitor the status and strength of the xenogeneic immune after transplantation.

Immortalized PTECs were genetically engineered with lentiviral vectors encoding for short hairpin (sh) RNAs targeting beta-2-microglobulin (β2m) and class II transactivator (CIITA) showed a silencing effect on β2m, CIITA, and SLA-DRα mRNA transcript levels of 84.66% ± 0.049 (P < 0.0001), 80.47% ± 0.076 (P < 0.0001) and 79.58% ± 0.044 (P < 0.0001), respectively, compared to cells transduced with lentiviral particles encoding for non-specific shRNA (shNS) (Fig. 5a). Correspondingly, in comparison to SLA-expressing (shNS) imPTECs, the silencing effect on the β2m and CIITA at RNA levels was translated into

a downregulation on SLA class I and class II surface expression of 97.02% ± 0.70 ($P < 0.0001$) and 34.96% ± 4.81 ($P = 0.0004$), respectively (Fig. 5b,c).

3.5 SLA-silenced PTECs induce weaker xenogeneic T-cell responses

T-cell-mediated cytotoxicity is a crucial evaluation parameter of the strength of xenogeneic immune responses. Even a reduced number of xenoreactive T-cells can potentially initiate a strong cellular response followed by organ rejection [19,20]. Our results show that the T-cell cytotoxic activity is decreased in the presence of SLA I and II silenced PTECs compared to the SLA expressing (non-transduced or shNS) PTECs. SLA class I and class II silenced cells showed higher cell survival rates than control groups after the exposition to xenoreactive T-cells. The normalized cell index of SLA-downregulated PTECs was significantly increased ($P = 0.0154$ at 20 hours, $P = 0.0008$ at 24 hours, $P = 0.0003$ at 28 hours, $P < 0.0001$ at 32 hours, $P = 0.0002$ at 36 hours, and $P = 0.0069$ at 40 hours) in comparison to SLA-expressing (shNS) PTECs. For instance, after 32 hours, the mean normalized cell index of the SLA class I and class II silenced PTECs (shβ2m + CIITA) was increased 3.33 fold and reached their maximum cell index after 28 hours. Remarkably, after 48 hours, the survival rate of silenced PTECs (shβ2m + CIITA) was still increased compared to the control groups (Fig. 6a). These data suggest that the use of imPTEC is suitable to access xenoreactive T-cell cytotoxicity and that silencing SLA expression protects renal epithelial cells against T-cell mediated lysis.

Cytokines are important immunomodulators in the context of xenotransplantation providing information on the status of immune responses after transplantation [21]. Thus, we characterized the cytokine secretion profile of xenoreactive T-cells after exposure to fully SLA-expressing or SLA-silenced imPTECs in vitro. Levels of all measured cytokines were decreased in cultures supernatants of SLA-silenced (shβ2m + CIITA) PTECs exposed to xenoreactive T-cells compared to those from transduced cells with the control shNS (Fig. 6b). Remarkably, cytokine secretion of IFN-γ and IL-6 were significantly reduced to 280.2 pg/mL (IFN-γ, $P < 0.0001$) and 5.52 pg/mL (IL-6, $P = 0.0056$) in supernatants where silenced PTECs (shβ2m + CIITA) were used as a target in comparison to those from cultures using shNS expressing PTEC (IFN-γ, 1550.35 pg/mL and IL-6 pg/mL 59.84). These results suggest that silencing SLA expression on renal tubular epithelial cells might contribute to decreasing the strength of xenogeneic immune responses targeting the pig kidney. In addition, these assays indicated that the generation of imPTECs is a robust strategy to generate sufficient material to reproducibly monitor the strength of the immune response.

3.6 NK cell cytotoxicity

Also, NK cell activity may play a relevant role in the survival of xenografts. NK cell cytotoxic activity might be activated due to the absence of inhibitory ligands such as MHC class I molecules or upon the binding of xenograft-specific antibodies [22]. Here, we investigated whether silencing the expression of SLA class I on renal cells and in particular on PTECs increases the susceptibility to NK cell cytotoxicity. Hence, the generated immortalized SLA-silenced porcine PTECs were co-cultured with human NK cells. Since resting

NK cells retain CD107a predominantly in their intracytoplasmic granular membranes, detection of CD107a on the cell surface is associated with cytotoxic activation and degranulation. [21,23].

Interestingly, reduced SLA expression in silenced PTECs did not increase the NK cell surface expression of CD107a (Fig. 7a,b). Expression levels of CD107a on NK cell surface were comparable upon exposure to non-transduced (18.30% ± 7.06), non-silenced (shNS, 15.73% ± 5.43), or SLA-silenced (shβ2m + CIITA, 19.33% ± 5.00) PTEC targets. Altogether, CD107a expression levels showed no significant differences between SLA-silenced PTECs in comparison to the SLA-expressing control groups. These results suggest that silencing of SLA class I expression does not induce xenogeneic NK-cell activation targeting renal epithelial cells.

Discussion

The use of porcine organs for xenotransplantation may enlarge the organ pool available to treat patients suffering from ESRD [24]. However, histocompatibility hurdles between the porcine organs and the human recipients need to be minimized or circumvented to support the success of this therapy [7]. Remarkable progress in the field of xenotransplantation has been achieved generating enormous advances [8,9]. In particular, the generation of genetically engineered pigs leads to significant improvements in xenograft survival [25]. Nevertheless, the immunological discrepancies between both species still pose a relevant hurdle by triggering immune rejection. In addition, based on phenotypic properties, specific cell types constituting the different organs may exhibit various levels of immunogenicity and are capable to trigger xenogeneic immune responses with different strengths [7]. Therefore, it is highly desirable to develop robust in vitro assays to investigate the feasibility and potency of specific genetic modifications on porcine cells in the regulation of xenogeneic immune responses.

Furthermore, in vitro assays may allow the prediction of the xenogeneic immune response targeting a specific organ and support the development of adequate immunosuppression regimens. Precise in vitro prediction of human immune responses also may allow the reduction of the number of non-human primates used in pre-clinical studies [26]. As the kidney is one of the most transplanted organs, we focused on the generation of renal epithelial cell lines that could be used to develop immunological assays as well as to serve as the basis of biotechnological platforms to evaluate the effect of specific genetic modifications and their impact on the strength of the human xenogeneic responses [27]. Here, we generated three PTEC lines and focused on their role in immune responses that may occur after kidney xenotransplantation.

SV40 large T-ag binds protein products of p53 and retinoblastoma genes and inactivates SEN6 [28]. The inactivation of Rb-proteins leads to the activation of transcription factor E2F, which initiates S-progression and promotes immortalization and proliferation [29]. It has already been reported that the rate of cell proliferation is related to the frequency of cells in different cell cycle phases. Flow cytometry analyses of the S-phase showed to be most useful to assess the cell proliferative capacity [30]. In our

study, SV40 large T-ag supported a steady proliferative capacity of PTECs without significant alteration of morphology and phenotype. However, other strategies to generate immortalized cells have been also described. For instance, the expression of the human telomerase reverse transcriptase (hTERT) or adenovirus early region 1A (E1A) gene has been widely used to generate cell lines [31].

Furthermore, to evaluate if SV40 T-ag expression affects PTEC functionality, we tested their capacity to migrate. Previous studies have shown that epithelial cells, especially after injury, exhibit a high capacity for tissue repair and regeneration compared to their healthy state in which they are mitotically quiescent [11,12]. In the kidney, this repair function is not provided by identifiable stem cell populations as compared to organs with high rates of cell turnover. Instead, the resident tubular cells dedifferentiate into potential progenitors for self-repair and proliferate after injury. Consequently, through their increasing mitotic activity of progenitor cells, they participate in wound healing processes after transplantation [14,32].

Generated imPTEC lines showed an increased migratory capacity even in higher passages in comparison to primary PTECs, suggesting that they maintain their cell functionality despite immortalization. The maintenance of renal PTEC typical phenotype and properties demonstrates their suitability for the development of in vitro testing assays.

Primarily, we generated those cell lines to characterize and predict potential human xenogeneic immune responses toward kidney tubular epithelial cells. Due to the genetic discrepancy between the different species, rejection often occurs. This problem has been reduced by the development of genetically modified pig kidneys. In addition to the prevention of hyperacute rejection by alpha-1,3-galactosyltransferase knockout pig kidneys, there is a multitude of candidate targets that might contribute to minimize the immune response against the xenograft [33]. Immortalized PTECs might play a relevant role in the evaluation of the potency of newly developed genetic modifications and allow the selection of the most effective.

In previous studies, we and others have shown the potential of silencing MHC expression to prevent immune responses. Recently, MHC knockout pigs were generated to provide organs with the capacity to evade immune responses after organ xenotransplantation [16,34]. In the allogeneic transplantation model, silencing MHC expression in different cell types, tissues and organs showed to be feasible and contributed to decreasing the susceptibility to antibody-mediated cellular and complement-dependent cytotoxicity. Furthermore, silencing MHC expression showed to induce weaker T-cell allogeneic immune responses and contribute to the significantly lower secretion of pro-inflammatory cytokines of IL-6 and IFN-γ [17,18,35,36]. IL-6 is involved in innate immune responses as well as adaptive immunity. The excessive release of IL-6 correlates with the activation of T-helper cells and the inhibition of regulatory T-cells, which may support an inflammatory response or autoimmune diseases after transplantation [37]. IFN-γ may directly act on kidney IFN-γ receptors supporting immune cell infiltration of the graft and amplification of the immune response. In addition, IFN-γ contributes to the upregulation of MHC on the graft [38]. Here, we could demonstrate that SLA-silenced PTECs could escape the specific T-cell cytotoxic attack and they also induced a reduced T-cell cytokine secretion. Accordingly to the results achieved in this study using

renal cells, Carvalho-Oliveira et al. also showed that the downregulation of SLA expression pancreatic beta-cells significantly decreases xenogeneic T-cell immune responses in vitro [39]. Hence, silencing SLA expression might represent a promising strategy to protect xenografts against T-cell responses.

Furthermore, xenogeneic NK-cell responses can be induced by the engagement of DSA bound to the target cell surface, the lack of self-MHC molecules, and the overexpression of activating ligands (e.g. NKG2D) or FASL- FAS interaction. Target cell recognition induces NK-cell cytotoxic attack by the release of lytic granules containing cytotoxic molecules such as perforins and granzymes as well as the secretion of pro-inflammatory cytokines (e.g. IFN-γ, TNF-α) [22,40]. The lack of MHC class I molecules on the surface of target cells induces the activation of NK cells and cytotoxic activity. [41] Here, the genetic modification of imPTECs demonstrated that silencing SLA class I and class II expression do not cause an upregulation of NK-cell degranulation, suggesting that the remaining SLA class I expression is sufficient to prevent NK-cell activation.

In conclusion, we demonstrated that imPTECs are suitable to develop immune assays aiming at the evaluation of the strength of the human immune response against porcine PTECs. We showed that transduction of primary PTECs with SV40 large T-ag is an efficient strategy to increase their lifespan without compromising their phenotype or function and may pave the development of robust immunomonitoring assays. Remarkably, silencing SLA class I and class II expression showed to reduce porcine PTEC immunogenicity leading to weaker xenogeneic immune responses. Hence, silencing SLA expression in the porcine kidney may represent a promising option to support graft survival in kidney xenotransplantation.

Materials And Methods

5.1 Isolation and phenotyping of PTECs

Animal experiments were approved by the supervisory authority (LAVES—Niedersächsisches Landesamt für Verbraucherschutz und Lebensmittelsicherheit) according to the recommendation of their Ethics Committee (LAVES, AZ 33.19-42502-04-16/2343) and conducted in compliance with the ARRIVE guidelines, the German animal welfare law, the German guidelines for animal welfare and the EU Directive 2010/63/EU. All experiments were performed in accordance with relevant guidelines and regulations.

Landrace pig kidneys were preserved on static cold storage since retrieval and during transport to the laboratory. Kidney biopsies were collected from the renal cortex and incubated for 1 hour at 37°C with collagenase type II (Gibco, Life Technologies Corporation, New York, USA). After biopsy digestion, the cell suspension was centrifuged and the cell pellet was resuspended in CnT-Prime Epithelial Cell Culture Medium (CnT-Prime Medium) (CELLnTEC ADVANCED CELL SYSTEMS AG, Bern, Switzerland) supplemented with penicillin-streptomycin 2% (C.C.Pro, Oberdorla, Germany) and seeded onto 6-well plates. The medium was replaced every second day.

Flow cytometry

Cell phenotyping was performed by analyzing typical PTEC markers. After performing intracellular staining using the IntraPrep Permeabilization Kit (Beckman Coulter, Krefeld, Germany), cells were incubated with primary antibodies anti-(AQP-1) monoclonal antibody (clone OTI2D10, MA5-25401, Invitrogen, Carlsbad, California, USA) followed by FITC-conjugated secondary antibody (clone RMG1-1, BioLegend) or anti-(ATP1A1) recombinant rabbit monoclonal antibody (clone ST0533, MA5-32184, Invitrogen) and anti-ZO-1 polyclonal antibody (61-7300, Invitrogen) followed by FITC-conjugated secondary antibody (BioLegend). Data acquisition was performed by BD FACSCanto™ II Clinical Flow Cytometer System (Becton, Dickinson & Company, New Jersey, USA) and results were analyzed using FlowJo software v10.6.2 (Becton, Dickinson & Company).

Immunofluorescent staining

PTECs were seeded into 8-well tissue culture chambers (Sarstedt, Nümbrecht, Germany). After reaching confluence, cells were fixed in 4% paraformaldehyde for 1 hour. Cells permeabilization was performed using 0.1% Triton X-100 (SIGMA-ALDRICH, Taufkirchen, Germany) and blocked with 1% Bovine Serum Albumin (Sigma-Aldrich Chemie GmbH) for 1 hour. Staining was performed for 1 hour using primary antibodies anti-(AQP-1) monoclonal antibody (clone OTI2D10, MA5-25401, Invitrogen) followed by FITC-conjugated secondary antibody (clone RMG1-1, BioLegend) or anti-(ATP1A1) recombinant rabbit monoclonal antibody (clone ST0533, MA5-32184, Invitrogen) and anti-ZO-1 polyclonal antibody (61-7300, Invitrogen) followed by FITC-conjugated secondary antibody (BioLegend). Cell nuclei were visualized using IS Mountain medium containing DAPI (Dianova, Hamburg, Germany) and incubated overnight at 4°C. Images were performed using Keyence BZ-8100E microscope (KEYENCE, Neu-Isenburg, Germany).

5.2 Lentiviral vector production

Immortalization of PTECs was performed using lentiviral vectors encoding for SV40 large T-ag and mCherry sequence as a reporter gene. Additionally, lentiviral vectors carrying the sequence for a secreted form of luciferase (NanoLuc) from Oplophorus gracilirostris and shRNAs targeting β2m and (CIITA), as well as a control vector encoding for a non-sense shRNA were produced as previously described. [42] Briefly, HEK293T cells cultured in HYPERFlask Cell Culture Vessels (Corning, New York, USA) in Dulbecco´s modified Eagle´s medium supplemented with 10% fetal calf serum (FCS), 2% penicillin-streptomycin and 1% glutamine were used for the production of all three vectors. HEK293T cells were co-transfected using polyethyleneimine (1 mg/mL) (Polysciences, Warrington, PA, USA) with lentiviral packaging plasmid psPAX2 and VSV-G envelope expressing plasmid pMD2.G, and shRNA-encoding lentiviral plasmid. After 48 hours of incubation, the cell supernatant was collected and centrifuged for 3 hours at 20.000 g at 16°C. Lentiviral vector pellets were resuspended in Williams´ Media E (Thermo Fisher Scientific, Waltham, MA, USA) and stored at -80°C until needed. For the titration, a p24 enzyme-linked immunosorbent assay (Cell Biolabs, San Diego, CA, USA) was performed.

5.3 Generation of proximal tubular epithelial cell lines

Three different PTEC lines were produced by transducing 80%-confluent primary PTECs monolayers in presence of 0.1% protamine sulfate with SV40 large T-ag encoding lentiviral vector carrying the gene sequence of mCherry as a reporter. After 24 hours, mCherry expressing PTECs were sorted using FACS Aria Fusion cell sorter (Becton Dickinson, New Jersey, USA). PTECs expressing the mCherry reporter gene were collected and expanded for further assays while non-transduced cells were used as control. mCherry-positive PTECs purity was evaluated by fluorescence microscopy using Keyence BZ-8100E microscope (KEYENCE, Neu-Isenburg, Germany). Likewise, flow cytometry analysis was performed using SA3800 Spectral Analyzer (Sony, Tokyo, Japan) by detecting mCherry fluorescence.

5.4 Immortalization efficiency

SV40 large T-ag expression levels were analyzed from primary cells (n = 3) at passages 0, 5, and 10, and immortalized cells (n = 3) at passages 0, 5, 10, 15, and 20. Total RNA was isolated using RNeasy Mini Kit (Qiagen, Hilden, Germany) and reverse transcribed to cDNA by High-Capacity cDNA Reverse Transcription Kit (Applied Biosystems, Foster City, USA). Quantitative real-time polymerase chain reaction (qRT-PCR) was performed using specific SV40 large T-ag primers (Fw: 5´-ACT CTT GCT TGC TTT GCT ATT TAC ACC AC-3´, Rv: 5´-TGT ATA GCA GTG CAG CTT TTT C-3´ and SV40 large T-ag probe 5´-ACT CTT GCT TGC TTT GCT ATT TAC ACC AC-3´) (TIB Molbiol Syntheselabor GmbH, Berlin, Germany).

5.5 Assessment of proliferation and cell cycle analysis

To determine the population proliferation rate, PTECs were passaged (ratio 1:2) once they reached confluence. This assay was performed in 12-well plates using CnT-Prime medium. Passages were counted for up to 40 days. To calculate the cell cycle state of primary and immortalized cells, three PTEC lines at low passages (passage 2) and high passages (passage 10) were examined. Cell cycle analysis was performed using Vybrant™ DyeCycle™ Violet Stain (Thermo Fisher Scientific) following the manufacturer's protocol. Therefore cells were stained for 1 hour and analyzed immediately after incubation time by flow cytometry.

5.6 Migration Assay

Migration assay was performed with primary and imPTECs at passage 2 or passage 10. 3x10^6 cells were seeded on 24-well flat-bottom plates and cultured in CnT-Prime medium. After 6 hours, a scratch (~ 300 µm) was made. Afterward, PTECs were cultured for 48 hours, and pictures were taken every 12 hours using a Lumascope 620 microscope (Etaluma, San Diego, CA, USA). Images were analyzed using Aperio ImageScope Software v12.4.0.5043 (Leica Biosystems, Deer Park, IL, United States).

5.7 Silencing SLA class I and class II expression

SLA class I and II downregulation was achieved by transduction with lentiviral vectors containing shRNA sequences targeting porcine β2m and CIITA. To evaluate the SLA class I and class II silencing effect, non-transduced, non-silenced (shNS), and silenced (shβ2m + shCIITA) PTECs were used. The silencing effect was evaluated at the mRNA level by qRT-PCR and protein level by flow cytometry after IFN-γ (50 ng/ml) for 48 hours.

Total RNA was isolated from three SLA-silenced PTEC lines and reversed transcribed using a High-Capacity cDNA Reverse Transcription Kit (Applied Biosystems). qRT-PCR was utilized to detect β2m, CIITA and SLA-DRα transcript levels were evaluated using Taqman assays: Ss03391156_m1 (Thermo Fisher Scientific), Ss06941905_g1 (Thermo Fisher Scientific), and Ss03389945_m1 (Thermo Fisher Scientific), respectively. GAPDH expression (Ss03375629_u1, Thermo Fisher Scientific) was used as an endogenous control.

SLA class I and class II protein expression was determined by flow cytometry. Cell staining was performed using an anti-SLA class I antibody (clone JM1E3, MCA2261, Bio-Rad Laboratories GmbH, Hercules, California, USA) and rat anti-SLA class II DQ antibody (clone K274.3G8, MCA1335, Bio-Rad Laboratories GmbH) followed by APC-conjugated anti-mouse IgG1 (clone RMG1-1, 406610, Invitrogen) or AlexaFluor488-conjugated goat anti-mouse IgG secondary antibody staining (A-11001, Invitrogen).

5.8 T-cell cytotoxicity assay

Human peripheral blood mononuclear cells (PBMCs) were isolated from five healthy donors by density gradient centrifugation using Lymphosep (c.c.pro GmbH, Oberdorla, Germany). T cells (effector cells) were isolated using magnetic-activated cell sorting of human Pan T cell isolation Kit (Miltenyi Biotec, Auburn, USA). Effector cells were co-cultured with non-transduced cells, non-silenced (shNS) and SLA-silenced (shβ2m + CIITA) PTECs for 6 days in RPMI 1640 medium (Lonza, Basel, Switzerland) supplemented with 5% human serum AB (c.c.pro GmbH) and IL-2 (100 U/ml) in a ratio of 1:5 (target: effector cells). PTECs (target cells) proliferation was continuously monitored using the xCELLigence Real-Time Cell Analyzer (Agilent Technologies, California, USA). Microtiter plates (E-Plates©) (Agilent Technologies, California, USA) were utilized to measure noninvasive electrical impedance. Cell index values were recorded every 5 minutes during the initial hour followed by measurements every 30 minutes until the experiment was terminated after 2 days.

After reaching the end of the experiment (40 hours), the supernatant was collected, centrifuged at 1.500 rpm for 5 min, and stored at -80°C until analysis. GM-CSF, IFN-γ, MCP-1, IL-6, IL-8, IP-10, and MCP-1 levels were determined using MILLIPLEX Human Cytokine/Chemokine/ Growth Factor Panel A Magnetic Bead Panel and Luminex® 100/200 analyzer (Luminex Corporation, Austin, Texas, USA). According to the manufacturer’s instructions, standards and samples were prepared and cytokine concentrations were calculated by Xponent software version 3.1 (Luminex Corporation).

5.9 NK cell degranulation assay

Human NK cells were isolated from three healthy donors. Briefly, PBMCs were isolated by density gradient centrifugation using Lymphosep (c.c.pro GmbH, Oberdorla, Germany), and NK cells were collected using human NK cell isolation Kit (Miltenyi Biotec, Bergisch Gladbach, Germany). For NK cell degranulation analysis, non-stimulated or 48 hours IFN-γ (50 ng/ml) stimulated, non-transduced, non-silenced (shNS), and SLA-silenced (shβ2m + CIITA) imPTEC were used. Target cells were co-cultured with NK cells for 4 hours at 37°C incubators in a ratio of 1:5 (target: effector). After incubation time, NK cell populations were identified using FITC-conjugated anti-CD3 (clone UCHT1, 300440, BioLegend, San Diego, CA, USA) and

AlexaFluor647-conjugated anti-CD56 (clone B159, 557711, BD Pharmingen) antibodies. NK cell degranulation was evaluated by detecting the expression of CD107a using a PE/Cy7-conjugated anti-CD107a antibody (clone H4A3, 328617, BioLegend).

5.10 Statistical Analysis

All data are reported as mean ± standard deviation (s.d.). For comparison between the two groups, the student's t-test was used. Comparison between more than two groups was performed by two-way ANOVA. p-values < 0.05 were considered significant and α-level of 0.05 was determined. All statistical analyses were conducted using GraphPad Prism version 8 software (GraphPad Software Inc, San Diego, CA, USA).

Declarations

Acknowledgments

We are thankful for the excellent technical assistance to Susanne Aufderbeck, Yvonne Speidel, Beata Meyer. We appreciate the assistance of Dr. Anna Dragon during the xCELLigence Real-Time Cell Analyzer runs. We are thankful to the Refor the financial support of this study.

Author contributions

KS performed the experiments, analyzed and interpreted the data and contribute to writing the manuscript, **RS** contributed with crucial advice, **NW** retrieved and prepared the kidneys **EV** performed experiments; **BP** contributed with crucial material, **RB** contributed with crucial advice, and **CF** analysed and interpreted the data and contribute to writing the manuscript.

Data availability

All data will be provided upon reasonable request to the corresponding author.

References

1. van der Rijt, S., Leemans, J. C., Florquin, S., Houtkooper, R. H. & Tammaro, A. Immunometabolic rewiring of tubular epithelial cells in kidney disease. *Nat Rev Nephrol*, doi:10.1038/s41581-022-00592-x (2022).
2. Glorie, K. M. *et al.* Coordinating unspecified living kidney donation and transplantation across the blood-type barrier in kidney exchange. *Transplantation* **96**, 814-820, doi:10.1097/tp.0b013e3182a132b7 (2013).
3. Francis, A. *et al.* Survival after Kidney Transplantation during Childhood and Adolescence. *Clin J Am Soc Nephrol* **15**, 392-400, doi:10.2215/cjn.07070619 (2020).
4. Melandro, F., Del Turco, S. & Ghinolfi, D. Age disparities in transplantation. *Curr Opin Organ Transplant* **26**, 536-541, doi:10.1097/mot.0000000000000906 (2021).

5. Mustian, M. N. & Locke, J. E. Positive Crossmatch Kidney Transplantation: State of the Art and Future Perspectives. *Curr Pharm Des* **26**, 3460-3467, doi:10.2174/1381612826666200521141749 (2020).
6. Cooper, D. K. C. *et al.* Clinical Pig Kidney Xenotransplantation: How Close Are We? *J Am Soc Nephrol* **31**, 12-21, doi:10.1681/asn.2019070651 (2020).
7. Meier, R. P. H. *et al.* Recent progress and remaining hurdles toward clinical xenotransplantation. *Xenotransplantation* **28**, e12681, doi:10.1111/xen.12681 (2021).
8. Reardon, S. First pig-to-human heart transplant: what can scientists learn? *Nature* **601**, 305-306, doi:10.1038/d41586-022-00111-9 (2022).
9. Reardon, S. First pig kidneys transplanted into people: what scientists think. *Nature* **605**, 597-598, doi:10.1038/d41586-022-01418-3 (2022).
10. Smith, P. L., Buffington, D. A. & Humes, H. D. Kidney epithelial cells. *Methods Enzymol* **419**, 194-207, doi:10.1016/s0076-6879(06)19009-6 (2006).
11. Stamellou, E., Leuchtle, K. & Moeller, M. J. Regenerating tubular epithelial cells of the kidney. *Nephrol Dial Transplant* **36**, 1968-1975, doi:10.1093/ndt/gfaa103 (2021).
12. Rayego-Mateos, S. *et al.* Molecular Mechanisms of Kidney Injury and Repair. *Int J Mol Sci* **23**, doi:10.3390/ijms23031542 (2022).
13. Nguan, C. Y. & Du, C. Renal tubular epithelial cells as immunoregulatory cells in renal allograft rejection. *Transplant Rev (Orlando)* **23**, 129-138, doi:10.1016/j.trre.2009.02.003 (2009).
14. Velnar, T. & Gradisnik, L. Tissue Augmentation in Wound Healing: the Role of Endothelial and Epithelial Cells. *Med Arch* **72**, 444-448, doi:10.5455/medarh.2018.72.444-448 (2018).
15. Figueiredo, C. *et al.* Immunoengineering of the Vascular Endothelium to Silence MHC Expression During Normothermic Ex Vivo Lung Perfusion. *Hum Gene Ther* **30**, 485-496, doi:10.1089/hum.2018.117 (2019).
16. Sake, H. J. *et al.* Possible detrimental effects of beta-2-microglobulin knockout in pigs. *Xenotransplantation* **26**, e12525, doi:10.1111/xen.12525 (2019).
17. Yuzefovych, Y. *et al.* Genetic Engineering of the Kidney to Permanently Silence MHC Transcripts During ex vivo Organ Perfusion. *Front Immunol* **11**, 265, doi:10.3389/fimmu.2020.00265 (2020).
18. Valdivia, E. *et al.* Genetic Modification of Limbal Stem Cells to Decrease Allogeneic Immune Responses. *Front Immunol* **12**, 747357, doi:10.3389/fimmu.2021.747357 (2021).
19. Scalea, J., Hanecamp, I., Robson, S. C. & Yamada, K. T-cell-mediated immunological barriers to xenotransplantation. *Xenotransplantation* **19**, 23-30, doi:10.1111/j.1399-3089.2011.00687.x (2012).
20. Siu, J. H. Y., Surendrakumar, V., Richards, J. A. & Pettigrew, G. J. T cell Allorecognition Pathways in Solid Organ Transplantation. *Front Immunol* **9**, 2548, doi:10.3389/fimmu.2018.02548 (2018).
21. Crane, A. T. *et al.* Interspecies Organogenesis for Human Transplantation. *Cell Transplant* **28**, 1091-1105, doi:10.1177/0963689719845351 (2019).
22. Puga Yung, G., Schneider, M. K. J. & Seebach, J. D. The Role of NK Cells in Pig-to-Human Xenotransplantation. *J Immunol Res* **2017**, 4627384, doi:10.1155/2017/4627384 (2017).

23. Grudzien, M. & Rapak, A. Effect of Natural Compounds on NK Cell Activation. *J Immunol Res* **2018**, 4868417, doi:10.1155/2018/4868417 (2018).
24. Cooper, D. K. C. *et al.* Xenotransplantation-the current status and prospects. *Br Med Bull* **125**, 5-14, doi:10.1093/bmb/ldx043 (2018).
25. Sykes, M. & Sachs, D. H. Transplanting organs from pigs to humans. *Sci Immunol* **4**, doi:10.1126/sciimmunol.aau6298 (2019).
26. Langley, G., Evans, T., Holgate, S. T. & Jones, A. Replacing animal experiments: choices, chances and challenges. *Bioessays* **29**, 918-926, doi:10.1002/bies.20628 (2007).
27. Lewis, A. *et al.* Organ donation in the US and Europe: The supply vs demand imbalance. *Transplant Rev (Orlando)* **35**, 100585, doi:10.1016/j.trre.2020.100585 (2021).
28. Banga, S. S. *et al.* SEN6, a locus for SV40-mediated immortalization of human cells, maps to 6q26-27. *Oncogene* **14**, 313-321, doi:10.1038/sj.onc.1200842 (1997).
29. Giacinti, C. & Giordano, A. RB and cell cycle progression. *Oncogene* **25**, 5220-5227, doi:10.1038/sj.onc.1209615 (2006).
30. Golias, C. H., Charalabopoulos, A. & Charalabopoulos, K. Cell proliferation and cell cycle control: a mini review. *Int J Clin Pract* **58**, 1134-1141, doi:10.1111/j.1742-1241.2004.00284.x (2004).
31. Maqsood, M. I., Matin, M. M., Bahrami, A. R. & Ghasroldasht, M. M. Immortality of cell lines: challenges and advantages of establishment. *Cell Biol Int* **37**, 1038-1045, doi:10.1002/cbin.10137 (2013).
32. Guo, J. K. & Cantley, L. G. Cellular maintenance and repair of the kidney. *Annu Rev Physiol* **72**, 357-376, doi:10.1146/annurev.physiol.010908.163245 (2010).
33. Montgomery, R. A. *et al.* Results of Two Cases of Pig-to-Human Kidney Xenotransplantation. *N Engl J Med* **386**, 1889-1898, doi:10.1056/NEJMoa2120238 (2022).
34. Reyes, L. M. *et al.* Creating class I MHC-null pigs using guide RNA and the Cas9 endonuclease. *J Immunol* **193**, 5751-5757, doi:10.4049/jimmunol.1402059 (2014).
35. Valdivia, E. *et al.* Genetic Modification of Limbs Using Ex Vivo Machine Perfusion. *Hum Gene Ther*, doi:10.1089/hum.2021.199 (2022).
36. Börger, A. K. *et al.* Generation of HLA-Universal iPSC-Derived Megakaryocytes and Platelets for Survival Under Refractoriness Conditions. *Mol Med* **22**, 274-285, doi:10.2119/molmed.2015.00235 (2016).
37. Jordan, S. C. *et al.* Interleukin-6, A Cytokine Critical to Mediation of Inflammation, Autoimmunity and Allograft Rejection: Therapeutic Implications of IL-6 Receptor Blockade. *Transplantation* **101**, 32-44, doi:10.1097/tp.0000000000001452 (2017).
38. Hidalgo, L. G. & Halloran, P. F. Role of IFN-gamma in allograft rejection. *Crit Rev Immunol* **22**, 317-349 (2002).
39. Carvalho Oliveira, M. *et al.* Generating low immunogenic pig pancreatic islet cell clusters for xenotransplantation. *J Cell Mol Med* **24**, 5070-5081, doi:10.1111/jcmm.15136 (2020).

40. Maeda, A. *et al.* A Strategy for Suppressing Macrophage-mediated Rejection in Xenotransplantation. *Transplantation* **104**, 675-681, doi:10.1097/tp.0000000000003024 (2020).
41. Benichou, G., Yamada, Y., Aoyama, A. & Madsen, J. C. Natural killer cells in rejection and tolerance of solid organ allografts. *Curr Opin Organ Transplant* **16**, 47-53, doi:10.1097/MOT.0b013e32834254cf (2011).
42. Figueiredo, C. *et al.* Immunoengineering of the Vascular Endothelium to Silence MHC Expression During Normothermic Ex Vivo Lung Perfusion. *Human Gene Therapy* **30**, 485-496, doi:10.1089/hum.2018.117 (2018).

Figures

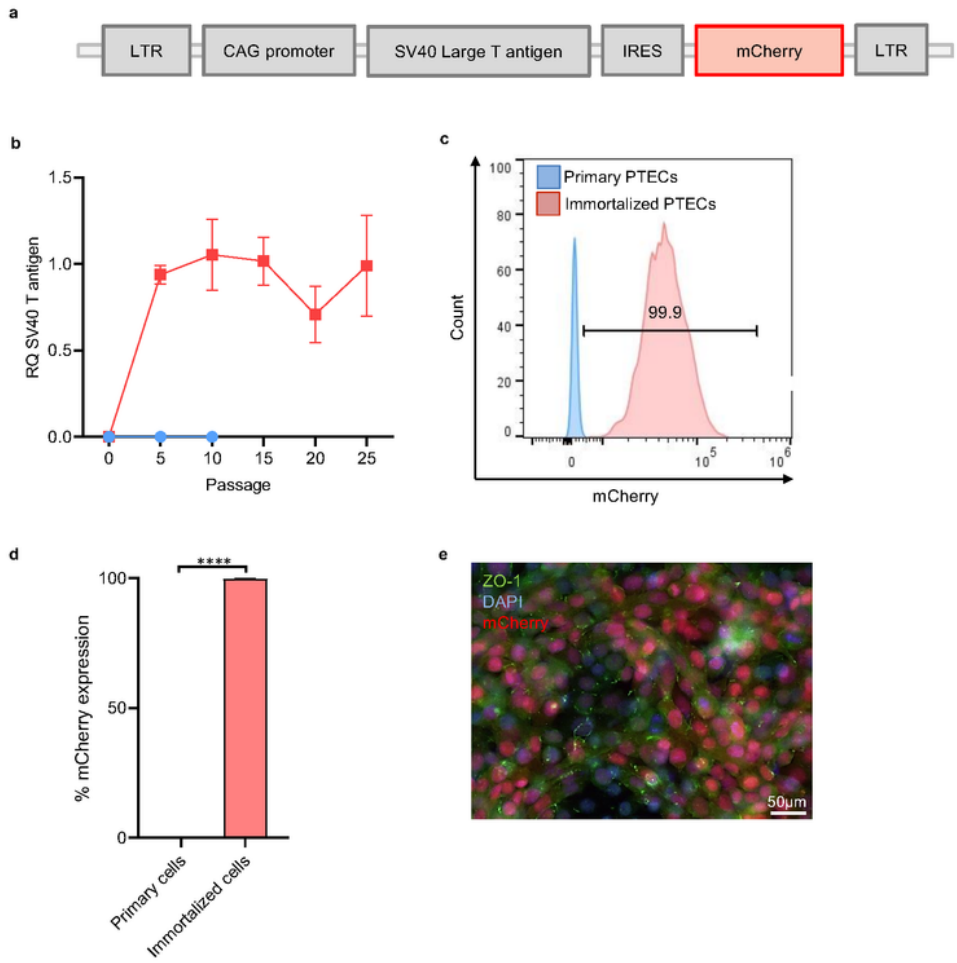

Figure 1

Immortalization of proximal tubular epithelial cells (imPTECs) by transduction using SV40 large T antigen (SV40 large T-ag)-encoding lentiviral vectors. (a) Schematic representation of the SV40 large T-ag encoding vector. **(b)** Relative quantification of SV40 large T-ag expression in primary and imPTECs. **(c)** Representative histogram of mCherry fluorescence of imPTECs. **(d)** Comparison of primary and imPTECs mCherry expression. Statistical significance was calculated by using an unpaired t-test. ****P<0.0001.

(e) Representative picture of PTECs expressing mCherry. PTEC nuclei were stained with DAPI (blue) and the tight junction protein-1 (ZO-1) marker is displayed in green.

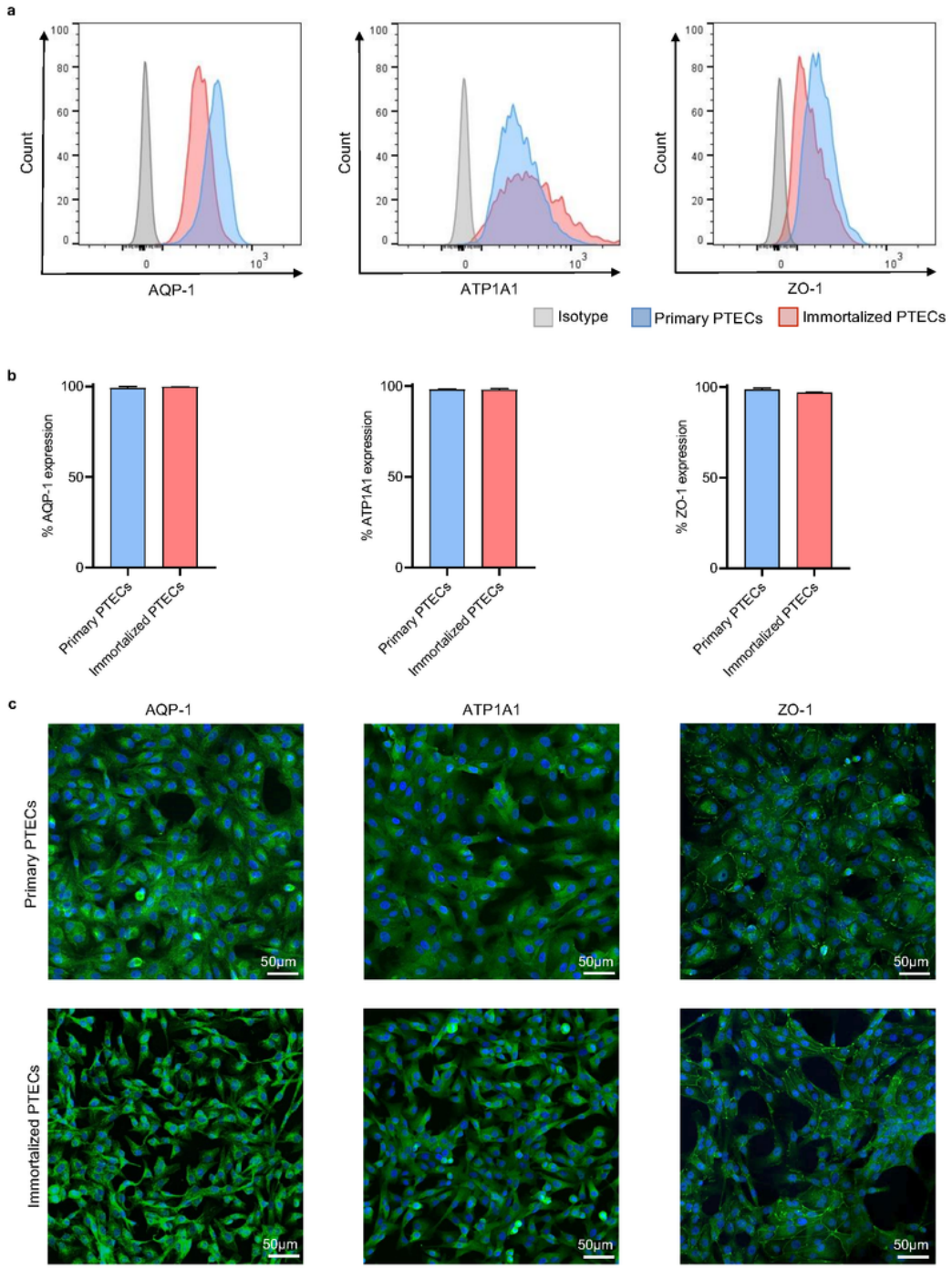

Figure 2

Phenotypic characterization of primary and immortalized PTECs. (a) Representative overlay histograms of aquaporin-1 (AQP1), sodium/potassium-transporting ATPase subunit alpha-1 (ATP1A1), and ZO-1

expression. **(b)**AQP1, ATP1A1, and ZO-1 mean expression (n=3). **(c)** Immunofluorescence analysis of specific proteins (AQP1, ATP1A1, and ZO-1) expressed on primary and PTEC lines. Marker expression is represented in green and DAPI in blue. Statistical analysis was evaluated by using an unpaired t-test.

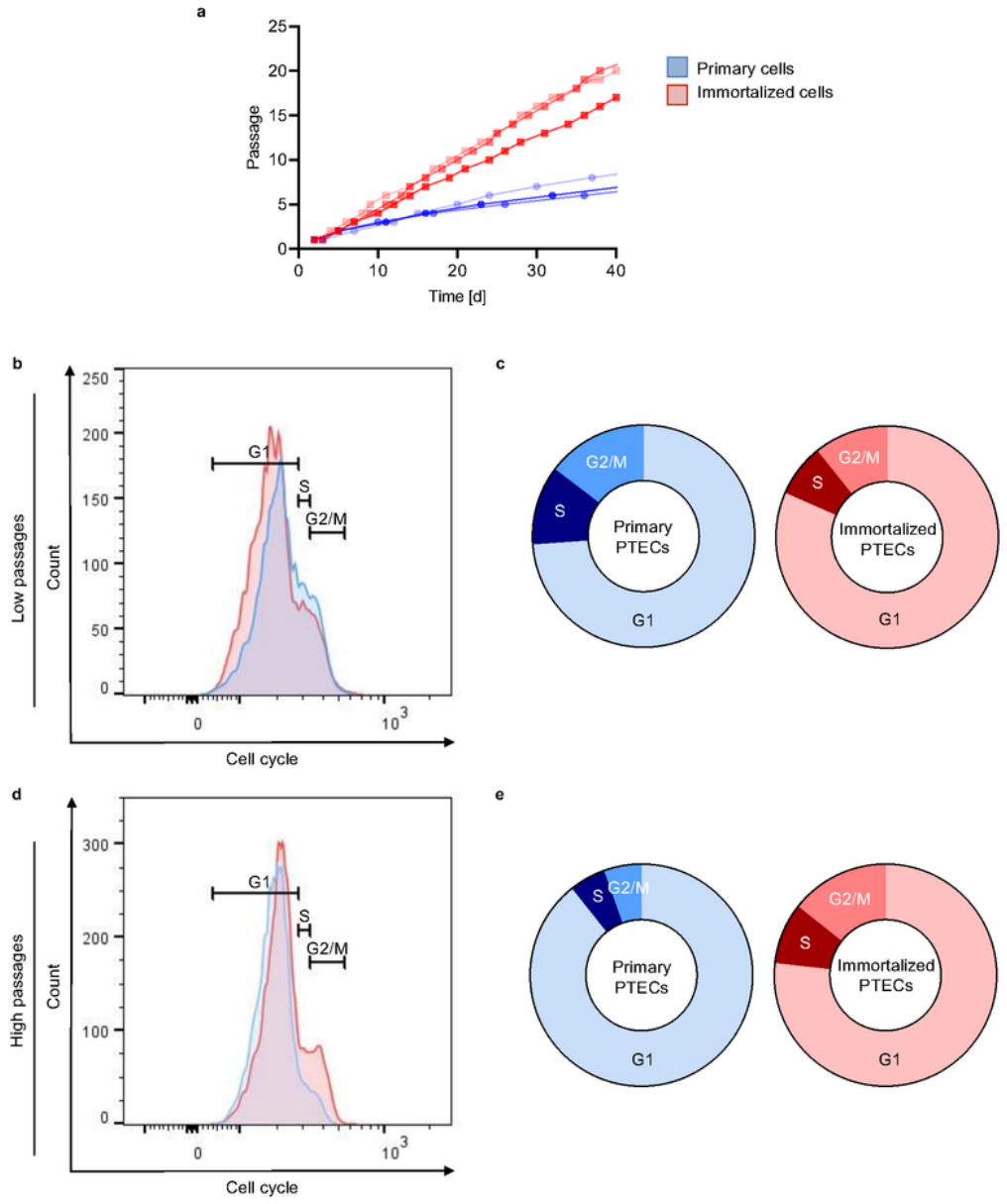

Figure 3

Immortalized PTECs (imPTEC) exhibit altered growth dynamics. (a) Doubling population analysis of primary and imPTECs (n=3). **(b)** Representative overlay histograms of cell cycling analysis of primary and immortalized cells in the low passage (passage 2) **(d)** and high passage (passage 10) **(c)** Proportion of primary and **(e)** imPTEC in each phase cycle stages. Statistical significance was calculated by using an unpaired t-test.

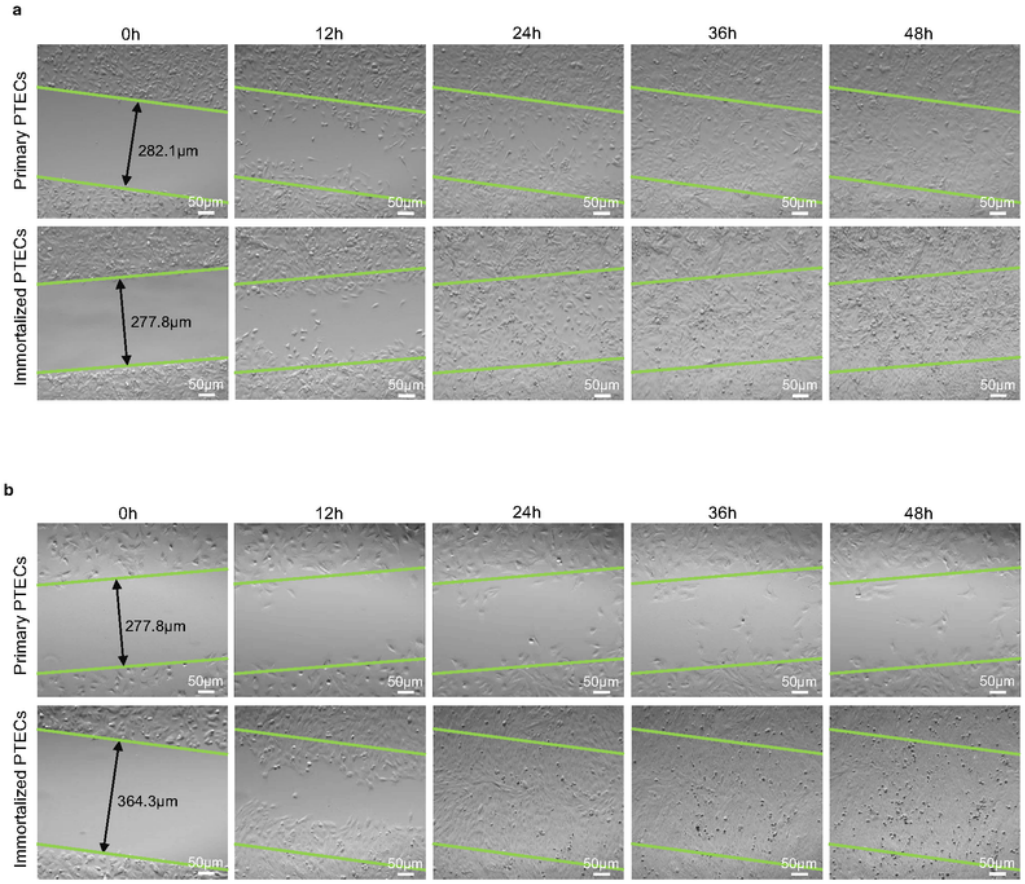

Figure 4

Immortalized PTECs (imPTEC) functional capacity remains constant even at high passages. The migration capacity of PTEC was evaluated in scratch assays. Pictures display time-lapse sequences of the capacity of primary and imPTECs to close gaps during a period of 48 h. Pictures were collected every 12 hours. **(a)** Representative images of PTECs in low passages (passage 2) and **(b)** in high passages (passage 10).

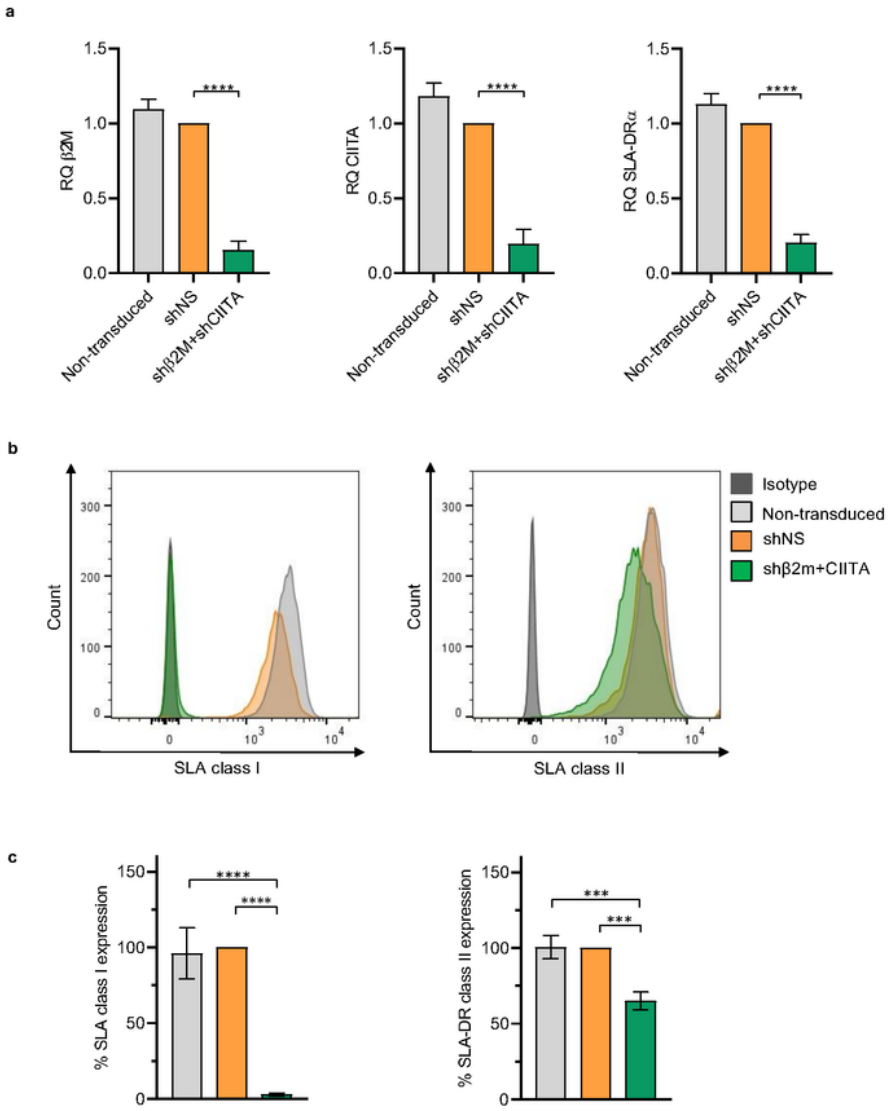

Figure 5

Silencing SLA class I and class II expression on immortalized PTECs (imPTEC). (a) Relative quantification of β2-microglobulin (β2m), class II transactivator (CIITA), and SLA-DRα transcript levels detected in non-transduced, non-silenced (shNS) and silenced (shβ2m+CIITA) imPTECs (n=3). Statistical significance was evaluated using two-way ANOVA. *P=0.0371, **P=0.0040, ****P<0.0001. **(b)** Representative histogram of SLA class I and class II expression levels on non-transduced, non-silenced (shNS) and silenced (shβ2m+CIITA) imPTECs (n=3). **(c)**Mean and standard deviation of SLA class I and class II expression levels on non-transduced, non-silenced (shNS), and silenced (shβ2m+CIITA) imPTECs. Statistical significance was evaluated using two-way ANOVA. Non-transduced compared with silenced PTECs. ***P=0.0004, ****P<0.0001.

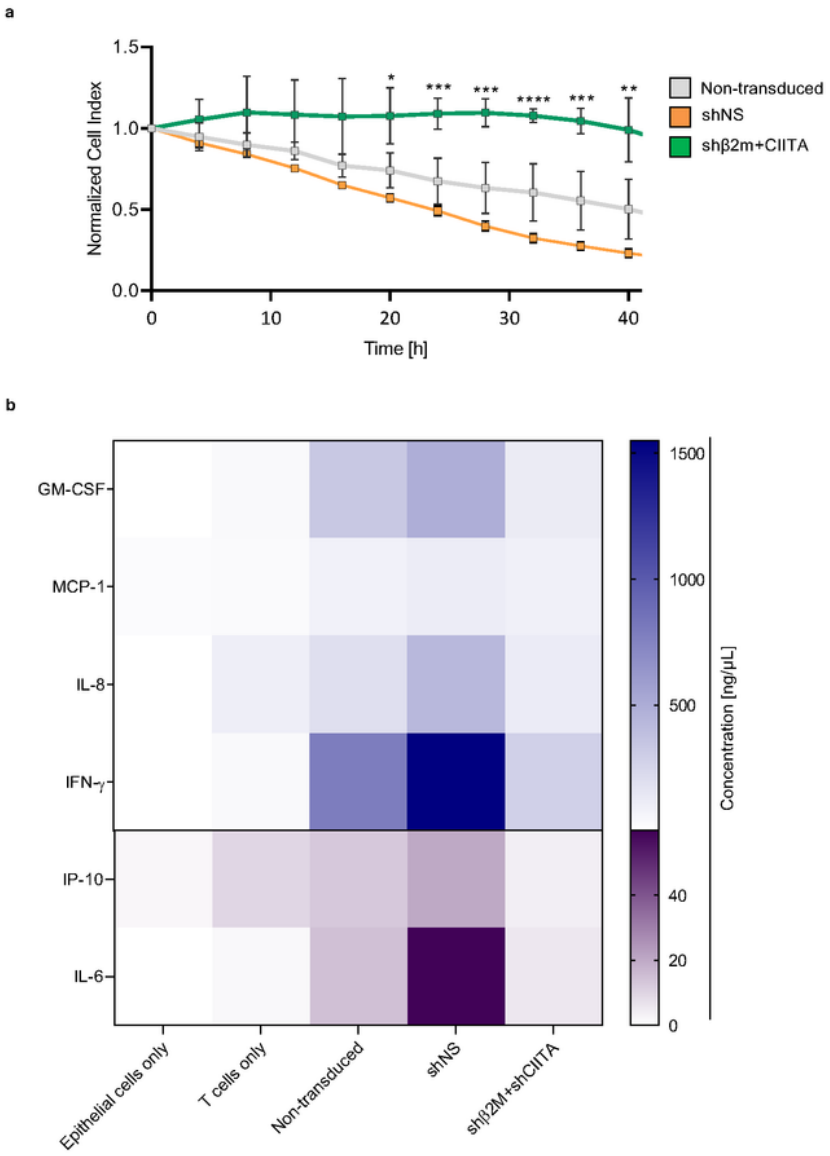

Figure 6

SLA class I and class II –silenced imPTECs are protected against xenogenic T-cell responses. (a) Normalized cell index of non-transduced, non-silenced (shNS), and SLA-silenced (shβ2m+CIITA) imPTECs incubated with primed xenoreactive T cells after 6 days of co-culturing. Statistical significance was calculated using two-way ANOVA. *P=0.0154 (20 hours), ***P=0.0008 (24 hours), ***P=0.0003 (28 hours), ****P<0.0001 (32 hours), ***P=0.0002 (36 hours), and **P=0.0069 (40 hours). **(b)** Heat map

represents xenoreactive T-cell cytokine secretion. Cytokine concentrations were detected after incubation of non-transduced, non-silenced (shNS), and SLA-silenced (shβ2m+CIITA) immortalized PTECs with human T cells.

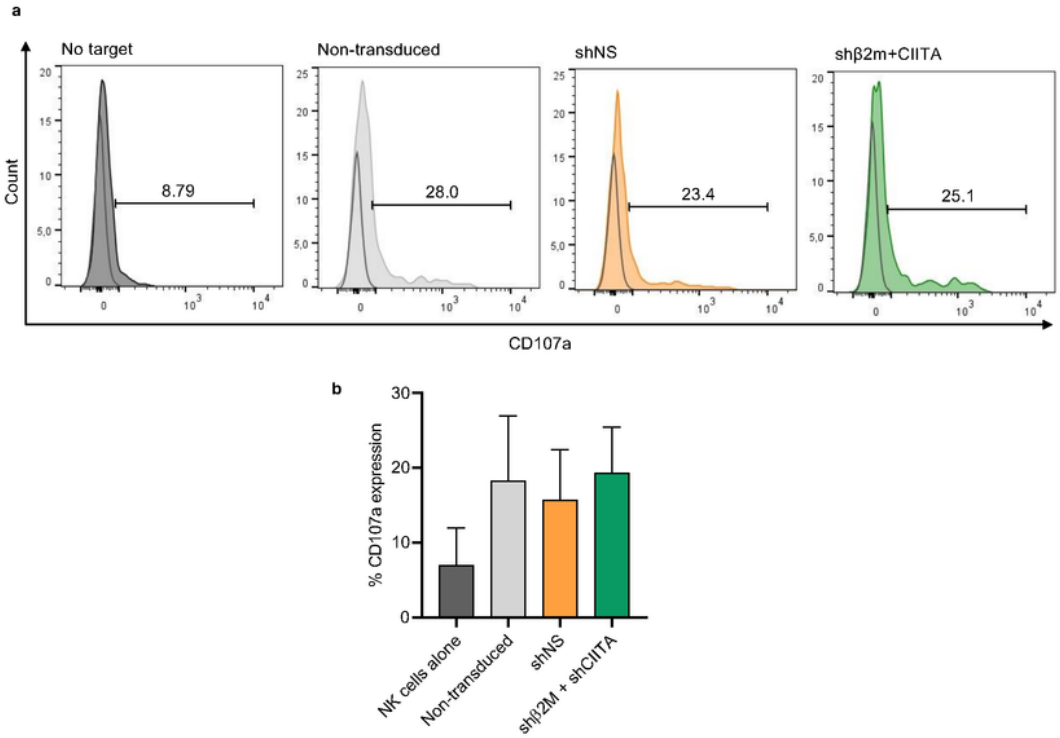

Figure 7

Silencing SLA class I expression on imPTECs does not trigger NK cell cytotoxicity. Expression levels of CD107a of immortalized SLA-expressing or SLA-silenced imPTECs were co-cultured with human NK cells for 4 hours, afterwards, levels of CD107a expression were measured by flow cytometric analysis. **(a)**Representative histogram plots of CD107a expression after NK cell exposure to no target (basal levels), non-transduced, non-silenced (shNS), and SLA-silenced (shβ2m+CIITA). **(b)** Mean and standard deviations of the levels of CD107a expression.